DESIGN OF MINIATURIZED ANTENNA FOR IOT APPLICATIONS USING METAMATERIAL

AHMAD ZAMANI JUSOH, NUR FATIHAH HUSAIN[*],
NORUN FARIHAH ABDUL MALEK, FARAH NADIA MOHD ISA,
AND SARAH YASMIN MOHAMAD

Department of Electrical and Computer Engineering,
Kulliyyah of Engineering
International Islamic University Malaysia,
Jalan Gombak, 53100 Kuala Lumpur, Malaysia

[*]Corresponding author: tihah0704@gmail.com

ABSTRACT: With the accelerated development of wireless technology, miniaturized antennae have become outstandingly favored due to the growing demand of Internet of Things (IoT) devices that are essential to accommodate low power, high data rates, and long-range communication. When an antenna operates at lower frequencies, the size of the antenna becomes bulky, which has raised an issue in the integration of the antennae within IoT devices due to their size constraints. Hence, in this paper, a miniaturized ring-monopole antenna incorporated with Rectangular Complementary Split Ring Resonator (RCSRR) and slotted ground plane, was designed at 2.4 GHz and 5.8 GHz frequency bands. The antenna was miniaturized by 46.8 % with overall size of 30 mm x 24.8 mm x 1.6 mm, and it was printed on FR-4 substrate with dielectric constant of 4.3. Design optimization was carried out by modifying the antenna structure, optimizing the dimensions, and using a low loss Rogers RT5880 substrate with a dielectric constant of 2.2, and thickness of 1.575 mm. The width of the antenna was also reduced to 20 mm which furthered the size reduction to 57.8 %. From the simulation results, the antenna was operated at 2.448 GHz, 2.864 GHz, and 5.8 GHz frequency bands with good return loss at -13.872 dB, -33.491 dB, and -19.3 dB respectively. The antenna fabrication and measurement were also implemented to the best simulated design using different substrates to validate its performance by comparing the simulated results with the measured results.

ABSTRAK: Dengan perkembangan pesat teknologi tanpa wayar, antena miniatur telah menjadi sangat digemari kerana permintaan yang semakin meningkat bagi peranti Internet Benda (IoT), iaitu mempunyai kuasa rendah, kadar data yang tinggi dan berkomunikasi jarak jauh. Apabila antena beroperasi pada frekuensi rendah, saiz antena menjadi besar, ini menimbulkan isu kekangan saiz pada antena ketika berada dalam peranti IoT. Oleh itu, kajian ini adalah berkenaan antena ekakutub-gelang kecil yang digabungkan dengan Resonator Gelang Pemisah Pelengkap Segiempat Tepat (RCSRR) dan satah tanah berslot, telah direka bentuk pada jalur frekuensi 2.4 GHz dan 5.8 GHz. Antena telah dikecilkan sebanyak 46.8 % dengan saiz keseluruhan 30 mm x 24.8 mm x 1.6 mm, dan ia dicetak pada substrat FR-4 dengan pemalar dielektrik 4.3. Reka bentuk optimum telah dilakukan dengan mengubah suai struktur antena, berdimensi optimum, menggunakan substrat Rogers RT5880 rendah kuasa dengan pemalar dielektrik 2.2, dan berketebalan 1.575 mm. Lebar antena juga dikurangkan sebanyak 20 mm, ini bermakna pengurangan saiz berjaya ditingkatkan kepada 57.8%. Dapatan simulasi menunjukkan antena telah beroperasi pada jalur frekuensi 2.448 GHz, 2.864 GHz dan 5.8 GHz dengan pengurangan kehilangan pulangan kuasa yang baik iaitu pada -13.872 dB, -33.491 dB

dan -19.3 dB masing-masing. Fabrikasi dan pengukuran antena juga telah dilaksanakan pada reka bentuk simulasi terbaik menggunakan substrat yang berbeza bagi mengesahkan kemampuannya dengan membandingkan dapatan simulasi dengan hasil yang diukur.

KEYWORDS: *miniaturized antenna; IoT application; metamaterial; complementary split ring resonator (CSSR).*

1. INTRODUCTION

Internet of Things (IoT) has been widely used in wireless applications such as wireless sensor networks, smart homes, and wearable technology [1]. This wireless technology requires persistent connectivity with the devices within its network to stay connected and to preserve its communication. To fulfil this need, Wi-Fi is attested to be the key requirement for IoT systems by providing numerous antennas for network connection. In 2019, the Wi-Fi Alliance launched the Wi-Fi CERTIFIED 6 based on IEEE 802.11ax standard to accommodate with IoT demand for low power, high data rates, and long-range communication [2]. However, Wi-Fi CERTIFIED 6 requires antennas that can operate at dual frequency bands of 2.4 GHz and 5 GHz which has created an issue in antenna integration within the devices due to its large size. Hence, various research has been conducted by scholars to develop diverse antenna miniaturization techniques to design compact antennae of distinct types such as patches, dipoles, loops, and slots that can satisfy the size constraints without degrading the performance of the antenna [3]. The many miniaturization techniques include adding slots [4], truncated and defected ground plane [5-8], meandered line [9], fractals [10] and metamaterial [11].

Metamaterial structure is a type of unnatural compound structure with physical characteristics that are distinct and novel from genuine elements and thus frequently used in designing a miniaturized antenna [12]. SNG metamaterial is a single negative material where either the value of permittivity, ε or permeability, μ is negative. Split Ring Resonator (SRR) is Mu-negative (MNG) metamaterial structure that consists of two metallic rings that can be designed in various shapes, such as square and circular, that are separated by a gap on opposite sides [12]. SRR unit cell is also equivalent to a circuit composed of inductor and capacitor which are represented by the rings and the gap between rings respectively [13].

Moreover, metamaterial structures can enhance the operation of the antenna on some parameters. In [14], DNG structure was constructed by making a 4 x 3 layer of metamaterial unit cells where it had 15 mm backlash space between the unit cells sheet and the substrate. This design of unit cells metamaterial improved the gain of the antenna from 1.48 dBi to 1.8 dBi and has good impedance matching with return loss of -52 dB. In [15], Complementary Split Ring Resonator (CSRR) form of metamaterial or the reciprocal split ring resonator, was designed at the front side of the patch antenna while at the back side, modified split ring resonator structure was designed. This enhanced the gain to 3.23 dBi, improved the bandwidth to 574 MHz, and reduced its size. Moreover, a square split ring resonator consisting of four metallic rings in [16], was able to exhibit resonant frequencies of different bands, making it especially useful in various applications. In this project, a miniaturized antenna incorporated with Rectangular Complementary Split Ring Resonator (RCSRR) and slotted ground plane, is designed, which accommodate a compact size of $0.2\lambda_0$ in term of its electrical length, and multi-band operation at 2.4 GHz and 5.8 GHz.

2. SLOTTED METAMATERIAL ANTENNA DESIGN

2.1 Preliminary Designs

Designing a miniaturized multi-band antenna requires the selection of a suitable miniaturization technique able to accommodate the required antenna characteristics while maintaining a good performance. Hence, metamaterial structure and slotted techniques are incorporated in the antenna design based on work by [17], where three design development steps were used to analyze its performance from each implementation of miniaturization techniques. A ring monopole antenna was initially designed with a size of 40 mm x 35 mm x 1.6 mm using the resonance frequency based on equation (1) [17].

$$f_r = \frac{c}{\pi C_1 \sqrt{\varepsilon_{eff}}} \tag{1}$$

where c refers to speed of light, $c = 3 \times 10^8$ m/s, C_1 is the outer diameter of the ring monopole ($C_1 = 2r_2$) and ε_{eff} is the equivalent dielectric constant. For FR4, $\sqrt{\varepsilon_{eff}} = 1.99, C_1 = 2r_2 = 18.9 \ mm$, then $f_r = 2.54$ GHz. For Rogers Duroid 5880, $\sqrt{\varepsilon_{eff}} = 1.48, C_1 = 2r_2 = 18.9 \ mm$, then $f_r = 3.4$ GHz.

First, antenna 1 was designed with the above parameters using CST Microwave Studio software [18]. The antenna was printed on FR-4 substrate with dielectric constant of 4.3 and loss tangent of 0.025. It was chosen as the substrate due to its easy accessibility. Then, the design was further developed by integrating Rectangular Complementary Split Ring Resonator (RCSSR) metamaterial structure as the radiating element. This development miniaturized the antenna to 30 mm x 24.8 mm x 1.6 mm which was approximately 46.8 % size reduction compared to conventional ring monopole. The changes in the near-field boundary conditions of the design had downsized the antenna to the targeted electrical length of $0.2\lambda_0$. The structure of the ground plane was kept similar as the previous design. This design produced a resonant frequency at 2.4 GHz which is the targeted operating frequency for Wi-Fi applications [19-22]. However, multi-band operation was not achieved from this design. Hence, L-shaped slots and a T-shaped slot were etched from the ground plane of the design to ensure multi-band operation. The addition of the slots altered the surface current distribution path to be longer, which made the antenna resonate at 2.32 GHz, 4.408 GHz, 6.34 GHz respectively. Nevertheless, the antenna had not yet achieved the targeted resonant frequencies at 2.4 GHz and 5.8 GHz. The illustration of the design development is depicted in Fig. 1 while the comparison of return loss characteristics of design development is shown in Fig. 2. The performance comparison of all preliminary designs (Antenna 1, Antenna 2, and Antenna 3) is summarized in Table 1.

2.2 RCSRR Metamaterial Design and Characteristic Verification

RCSRR, as depicted in Fig. 3, is the metamaterial structure consisting of two metallic rings as the radiating element with gaps between the rings and the split width on the opposite side of the rings. The split width of the rings was designed following the shape of capacitor to control its resonant frequency as it possesses the capacitance characteristics while the metallic rings possess inductance characteristics [17]. As a result of the applied outward H-field, an EMF is created around the RCSRR metamaterial structure, resulting in the coupling of the two rings. This happens due to the current travelling from outer ring to inner ring corresponding to the disperse capacitance by the split width of the rings Hence, RCSRR metamaterial structure behaves as an LC circuit [17]. RCSRR was positioned into the waveguide as illustrated in Fig. 4 where perfect electric conductor (PEC) and perfect magnetic conductor (PMC) boundary conditions were provided on the

y-axis and z-axis respectively to verify its characteristics. The boundary condition at the x-axis was set to open boundary to provide waveguides for both ports. The resonant frequency of RCSRR metamaterial structure can be ascertained using equation (2) where L_{tot} is the total inductance while C_{tot} is the total capacitance [17].

$$\omega_{r=} \frac{1}{\sqrt{L_{tot}C_{tot}}} \tag{2}$$

(a) Antenna 1   (b) Antenna 2
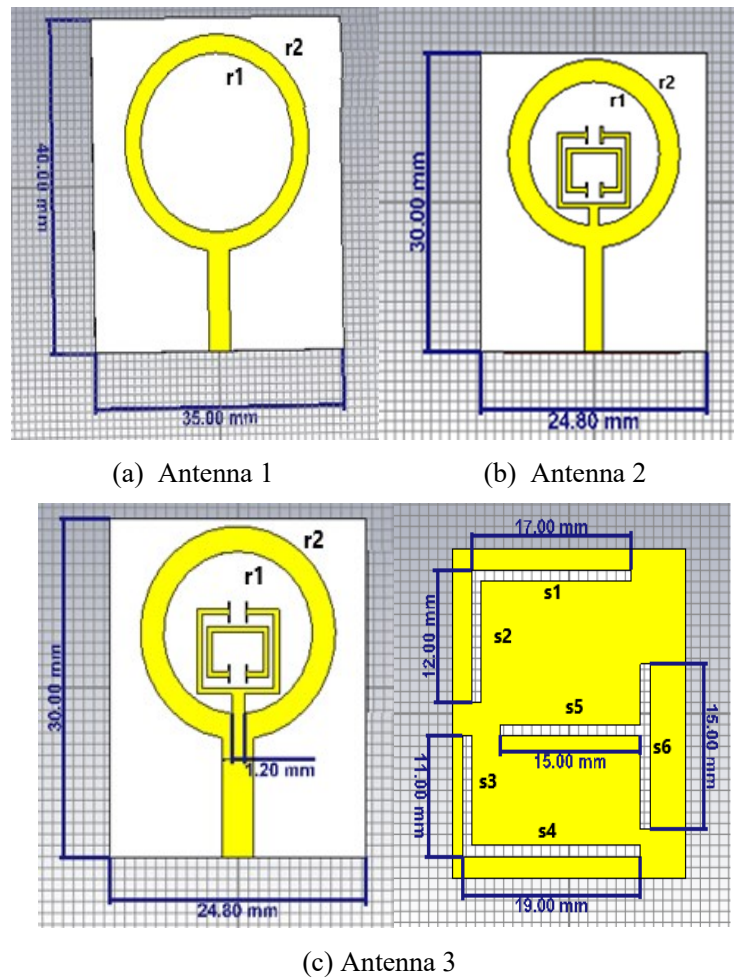
(c) Antenna 3

Fig. 1: Antenna design development.
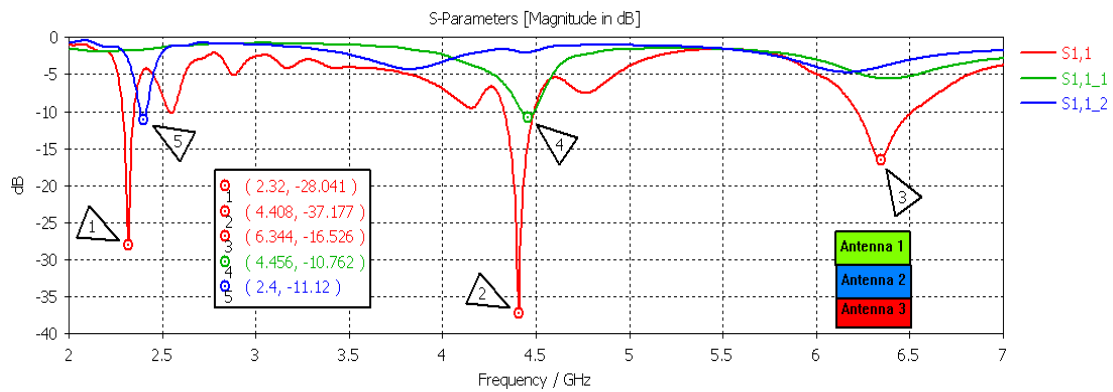
Fig. 2: Return loss characteristics of design development.

Table 1: Comparison of preliminary antenna designs

Antenna	Resonant frequency [GHz]	Size [mm^3]	Return loss [dB]
1	4.456	40 x 35 x 1.6	-10.762
2	2.4	30 x 24.8 x 1.6	-11.12
3	2.32, 4.408, 6.344	30 x 24.8 x 1.5	-28.041, -37.177, -16.526

From Fig. 5, it can be observed that the RCSRR unit cell that was positioned inside the waveguide medium had shown a stop band characteristic at 2.714 GHz. This is because, at this frequency, the value for S21or the transmission coefficient was below -10 dB and the value for the reflection coefficient or S11 was approaching 0 dB. Hence, a band notch was observed in the configuration of the return loss. Metamaterial structure is characterized by its negative value of permittivity or permeability depending on its type and RCSRR is categorized in Mu-negative metamaterial which indicates negative value of permeability as can be observed in Fig. 6, where the real value of permeability was negative at 2.714 GHz due to stop band characteristic of RCSRR. Therefore, negative permeability of RCSRR exhibits new resonance for the antenna. The dimensions of the RCSRR unit cell are: - a = 8 mm, b = 7.5 mm, c = 6 mm, d = 4.5 mm, s = 1.5 mm, g1 = 1 mm, and g2 = 0.5 mm.
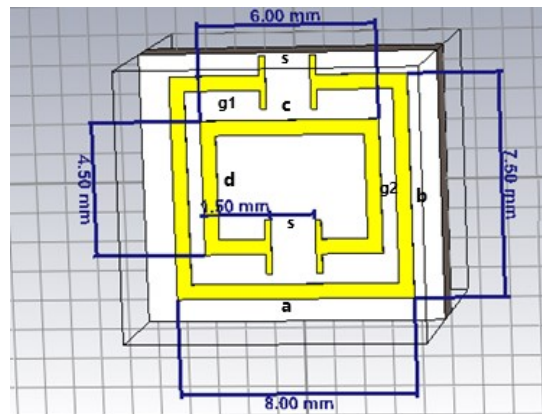
Fig. 3: RCSRR metamaterial structure.
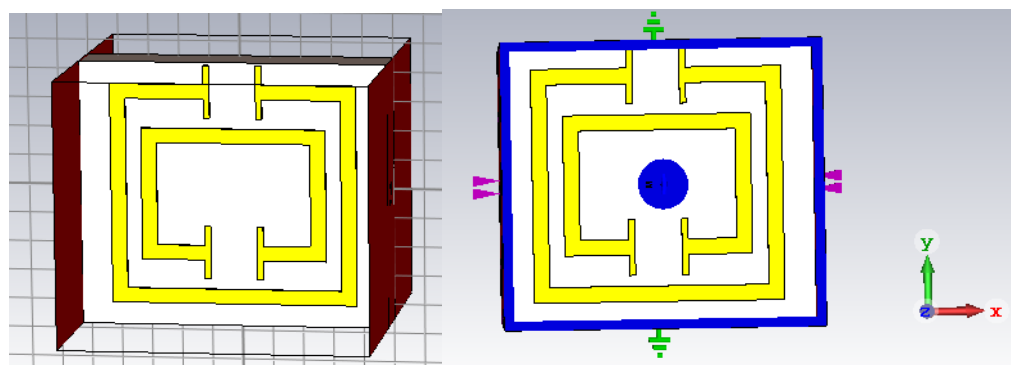
Fig. 4: RCSRR unit cell in waveguide medium with boundary conditions.
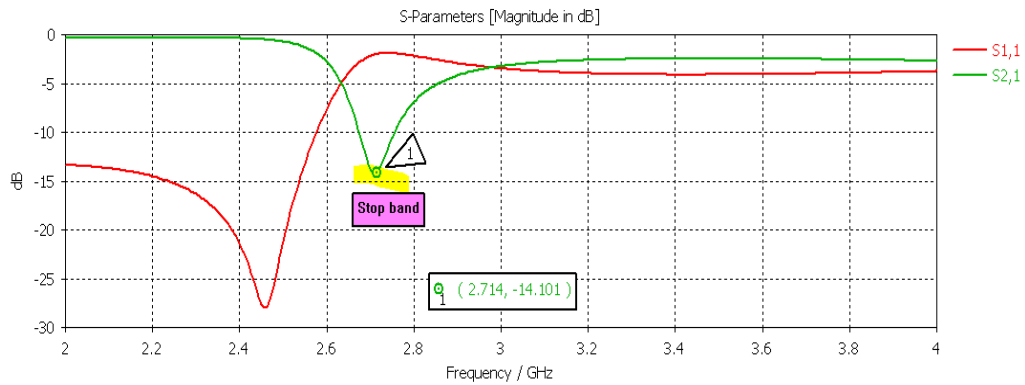
Fig. 5: Return loss of RCSRR unit cell.
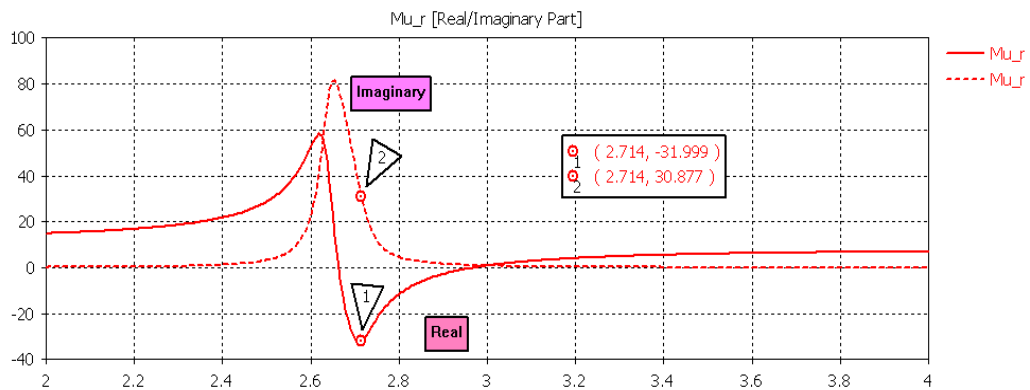
Fig. 6: Permeability of RCSRR unit cell.

2.3 Optimized Design

The preliminary antenna designs did not fulfill the targeted operating frequencies for Wi-Fi application to resonate at 2.4 GHz and 5.8 GHz. Thus, the design was optimized to ensure the best performance of the antenna. For antenna optimization, it is necessary to review its structure for performance enhancement by observing the effects of each addition of the slots to the ground plane. Hence, the T-shaped slot on the ground plane of Antenna 3 was eliminated from the design due to its effect in shifting the frequency to be greater than 2.4 GHz. After the modification to the ground plane structure, only two L-shaped slots were left for optimum radiation of the antenna.

Besides, parametric analysis was also carried out to some antenna dimensions to attain the best dimensions for the optimized design. The inner radius of the ring monopole, x was varied by a step of 0.05 mm as illustrated in Fig. 7. A value of x equal to 7.15 mm was chosen as the inner radius because it had good impedance matching at -19.487 dB compared to others. Then, the width of the connector between the ring monopole and RCSRR metamaterial structure, c was diversified by a step of 0.6 mm as depicted in Fig. 8. A value of c equal to 2.4 mm was selected as the best dimension because it had good return loss at -30.841 dB and its resonant frequency approached the targeted frequency of 2.4 GHz. Moreover, the length of the upper L-shaped slot, p was varied by a step of 0.5 mm as shown in Fig. 9. A value of p equal to 14.5 mm was used in the design as it had good impedance matching at -19.465 dB compared to others and it was able to resonate at approximately the targeted frequencies of 5.8 GHz. Other than that, the length of the lower L-shaped slot on the ground plane, q was altered by a step variation of 0.5 mm as depicted in Fig. 10. A value of q equal to 19.5 was selected as the best

dimension for q because it had good return loss at -21.777 dB compared to other dimensions. The complete optimized antenna design is illustrated in Fig. 11. The dimensions for optimized antenna design using FR-4 substrate (Antenna 4) are shown in Table 2.
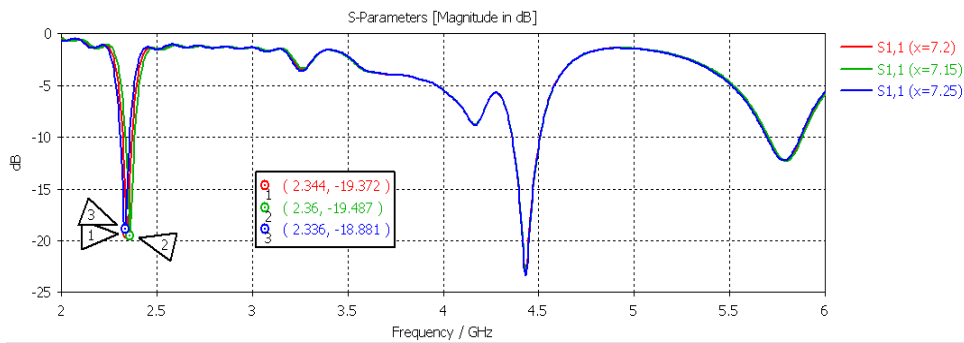
Fig. 7: Parametric analysis of the inner radius of ring monopole, x.
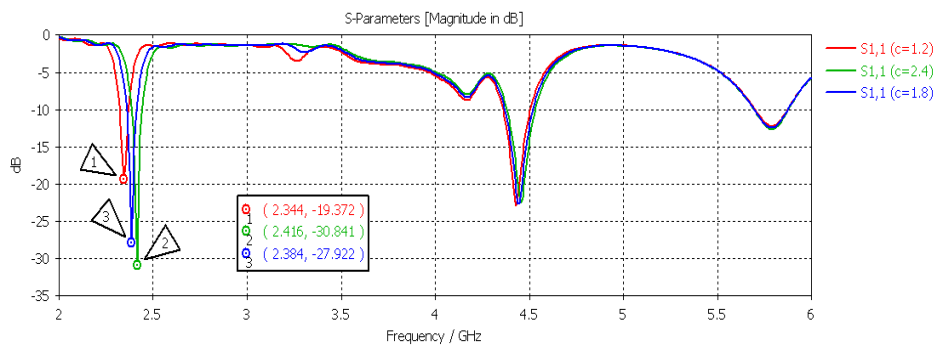
Fig. 8: Parametric analysis of the connector of feedline and RCSRR, c.
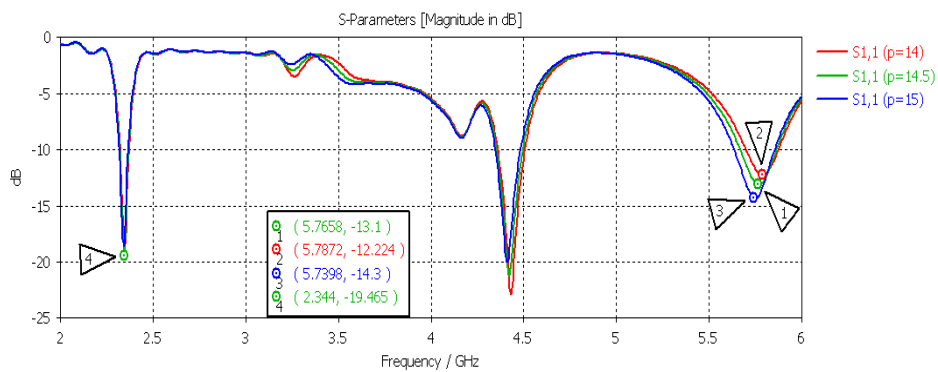
Fig. 9: Parametric analysis of the length of upper L-shaped slot, p.
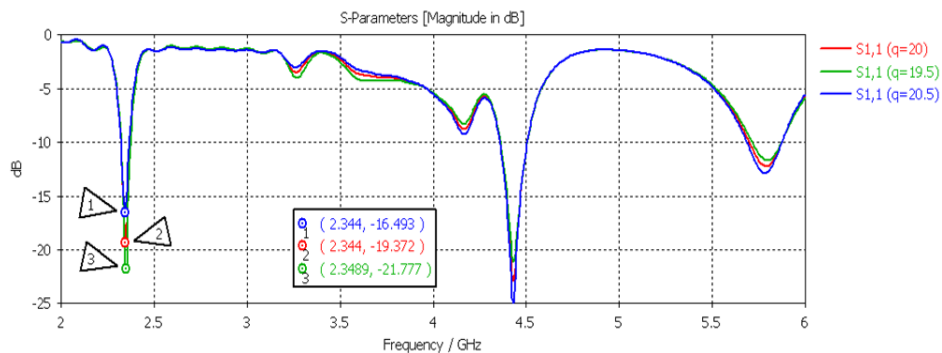
Fig. 10: Parametric analysis of the length of lower L-shaped slot, q.
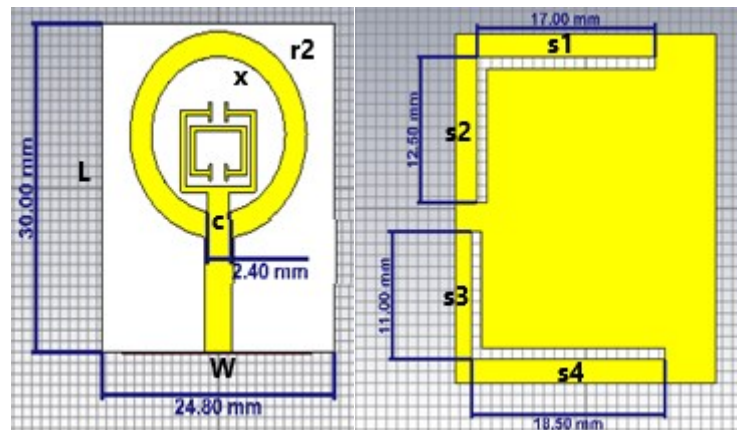
Fig. 11: Complete optimized antenna design using FR-4 substrate (Antenna 4).

Table 2: Dimensions of Antenna 4

Parameters	Unit (mm)
L	30
W	24.8
c	2.4
x (inner radius)	7.15
r2 (outer radius)	9.45
s1	17
s2	12.5
s3	11
s4	18.5

The dielectric material used in the design also affects the performance of the antenna. Hence, low loss dielectric material was considered in boosting the antenna performance. The antenna was designed on Rogers RT5880 substrate (Antenna 5), to replace FR-4. It has low dielectric constant equal to 2.2 compared to FR-4 that has high dielectric constant of 4.3 [17]. Moreover, the loss tangent of Rogers RT5880 substrate is 0.0009, which is also smaller than FR-4 with a loss tangent of 0.025 [17]. The complete optimized design of Antenna 5 is illustrated in Fig. 12 while its optimized dimensions are shown in Table 3. The optimized dimensions for RCSRR metamaterial structure incorporated in Antenna 5 is depicted in Fig. 13 where a = 9.5 mm, b = 8 mm, c = 6.5 mm, d = 5 mm, s = 1.5 mm, g1 = 1 mm, and g2 = 0.5 mm.
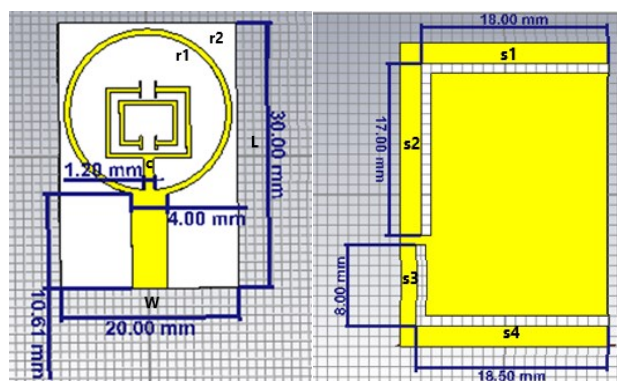
Fig. 12: Complete optimized antenna design using Rogers RT5880 substrate (Antenna 5).
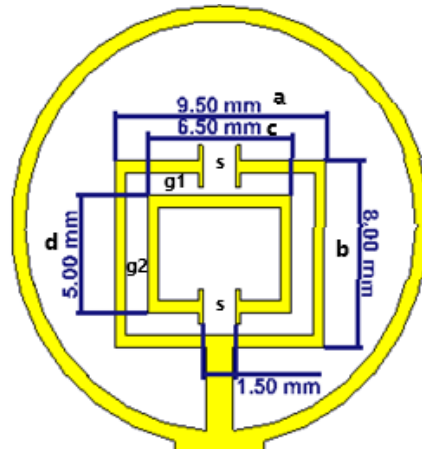
Fig. 13: RCSRR metamaterial structure optimized dimensions.

Table 3: Dimensions of Antenna 5

Parameters	Unit (mm)
L	30
W	20
c	1.2
r1 (inner radius)	8.8
r2 (outer radius)	9.45
s1	18
s2	17
s3	8
s4	18.5
Thickness	1.575

2.4 Antenna Fabrication and Measurement

The optimized antenna design printed on two different substrates, which are FR-4 and Rogers RT5880, were fabricated to validate the antenna performance by comparing the simulated result with the measured result. The fabrication was done at Mechatronics Workshop, Kulliyyah of Engineering, IIUM, where it involved six important steps: drilling the board to the required size, laminating the board using film, UV exposure, developing the required antenna design, etching the excess copper, and stripping the film residue [23]. An SMA connector was soldered on the antenna feedline for performance measurement. The complete fabricated antenna using two different substrates is depicted in Fig. 14. The measurement process was done at Microwave Lab using Vector Network Analyzer (VNA) as illustrated in Fig. 15.

3. OPTIMIZED DESIGN RESULTS AND DISCUSSION

Simulation of the design was conducted using CST Microwave Studio software. The optimized design using two different substrates of FR-4 (Antenna 4) and Rogers RT5880 (Antenna 5), were simulated. Some performance parameters were observed such as return loss, bandwidth, radiation pattern, directivity, and the gain to ascertain the best antenna performance for Wi-Fi application.

(a)

(b)
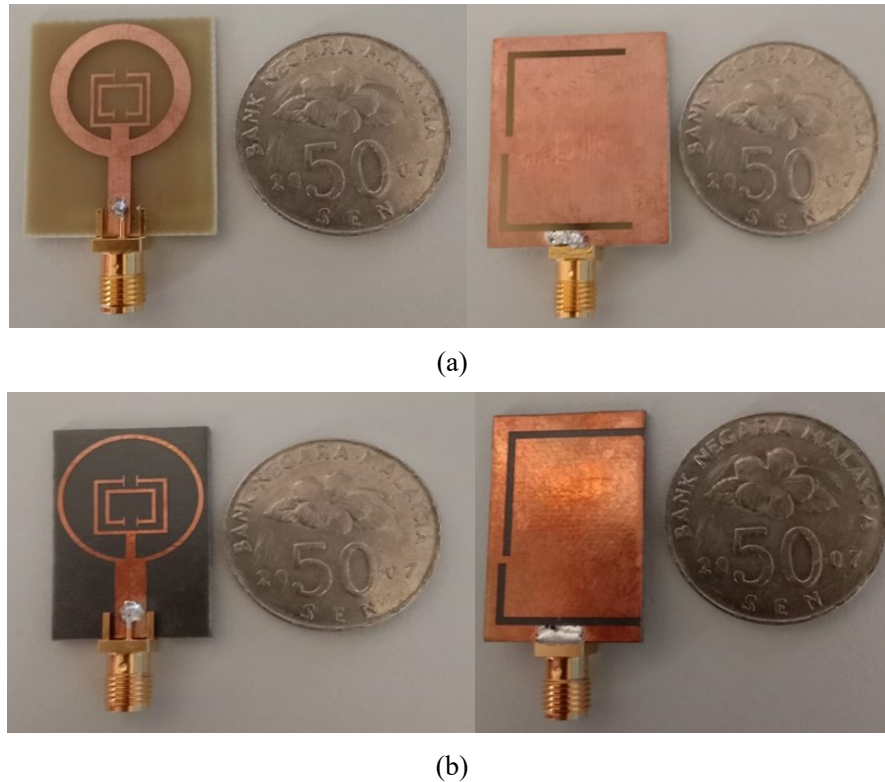
Fig. 14: Complete fabricated antenna using (a) FR4 substrate, (b) Rogers RT5880.

Fig. 15: Measurement of miniaturized antenna using Vector Network Analyzer.

3.1 Return Loss and Bandwidth

The important simulation data to be observed is the return loss (S11) or reflection coefficient. It is because it indicates the resonant frequency of the antenna and to evaluate whether the designed antenna will be able to operate at the targeted frequencies of both 2.4 GHz and 5.8 GHz. The acceptable value for S11 is below -10 dB which specified that 90 % power is transmitted to the antenna while 10 % of the power is being reflected. Bandwidth is the difference between the upper frequency and the lower frequency where it defined the frequency range covered for the operation of an antenna. It can be calculated using Eq. (3) where f_{upper} is the upper frequency, f_{lower} is the lower frequency, and f_0 is the centre frequency [1]. The -10dB bandwidth is considered in determining the bandwidth. The optimized design of slotted metamaterial ring monopole antenna using FR-4 substrate (Antenna 4) has good return losses of -27.102 dB, -20.864 dB, -13.517 dB at operating frequencies of 2.4 GHz, 4.44 GHz, and 5.8 GHz as depicted in Fig.16 with -10 dB bandwidth of 54.5 MHz or 2.27 %, 144.1 MHz or 3.25%, and 204.9 MHz or 3.53

%. Fig.17 shows the return losses of the optimized antenna design printed on Rogers RT5880 substrate (Antenna 5) which were -13.872 dB, -33.491 dB, and -19.3 dB at resonant frequencies of 2.448 GHz, 2.864 GHz, and 5.8 GHz respectively. It has -10 dB bandwidth of 137.2 MHz or 5.6 %, 350.9 MHz or 12.3 %, and 551.2 MHz or 9.5 % at respective resonant frequencies. The comparison between the return losses for antenna printed on two different substrates are depicted in Fig. 18 where both antennas achieved targeted resonant frequencies and had good impedance matching.

$$\text{Bandwidth} = \frac{f_{upper} - f_{lower}}{f_0} \qquad (3)$$
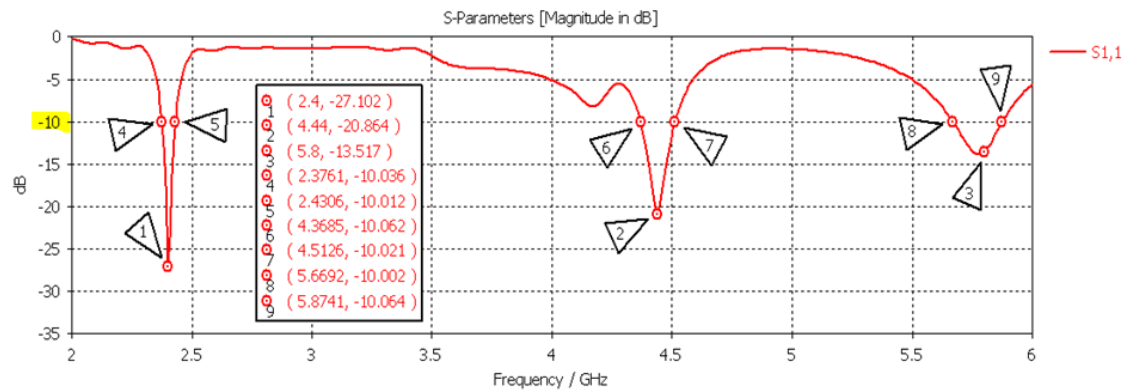
Fig. 16: Return loss of Antenna 4.
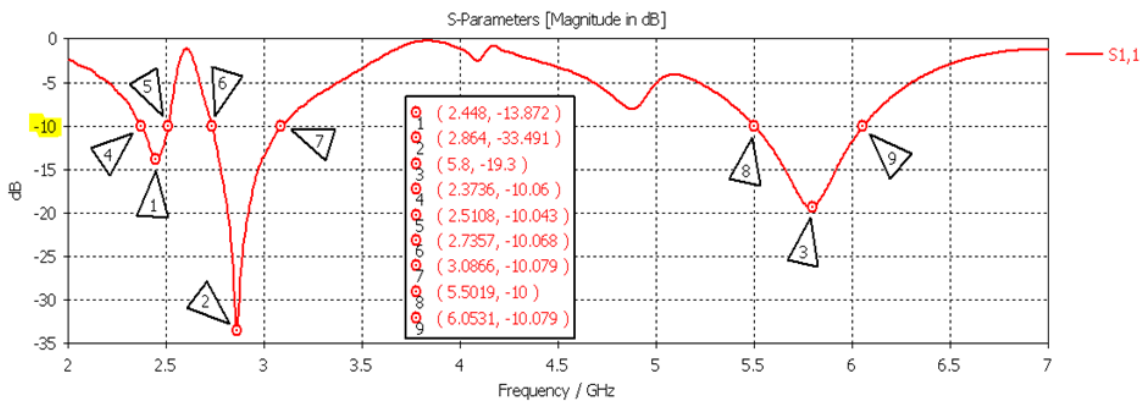
Fig. 17: Return loss of Antenna 5.
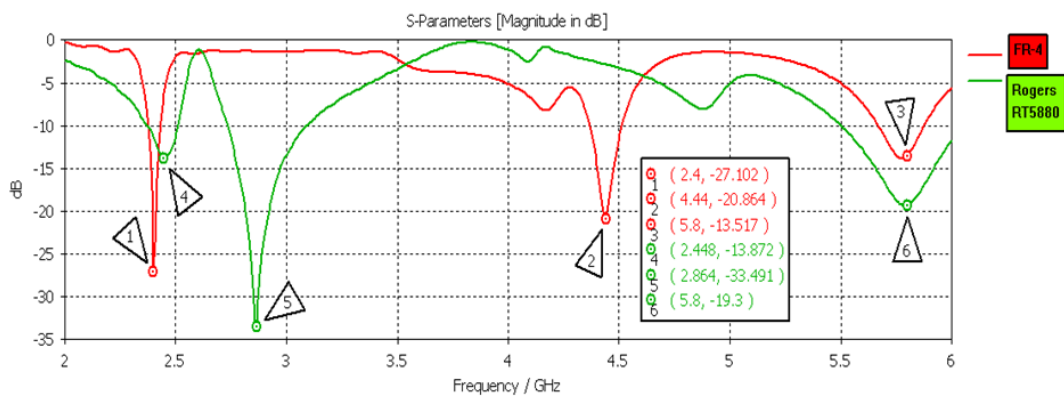
Fig. 18: Return loss comparison of antenna using different substrates.

3.2 Radiation Pattern

The 3D radiation patterns of Antenna 4 are illustrated in Fig. 19 where the patterns were directional at the respective operating frequencies. However, Antenna 5 had 3D radiation patterns that were almost omnidirectional patterns at resonant frequencies of 2.448 GHz and 2.864 GHz while at operating frequency of 5.8 GHz, the directional pattern, as depicted in Fig. 20, was seen. Hence, Antenna 5 is suitable for use in IoT applications since they require omnidirectional antennae and wider bandwidth for wireless connectivity [19-22]. The pattern considered was a far-field type and each pattern of all designs had different efficiencies and realized gains.

(a)   (b)   (c)
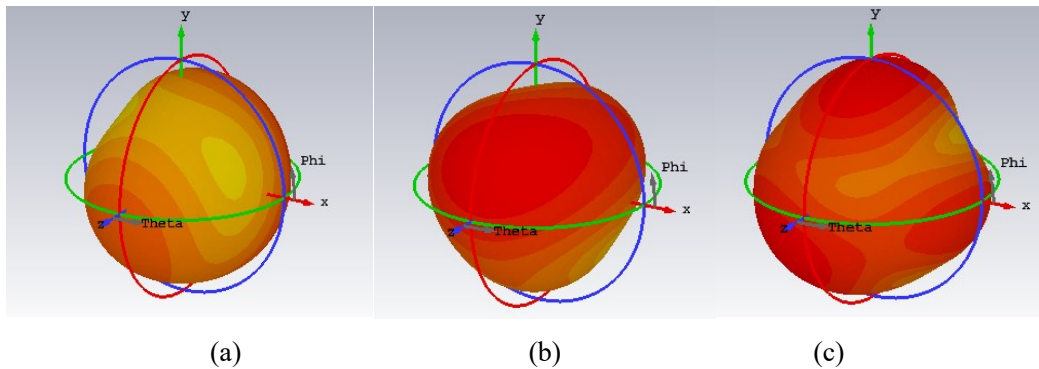
Fig. 19: 3D radiation pattern of Antenna 4 at (a) 2.4 GHz, (b) 4.44 GHz, (c) 5.8 GHz.

(a)   (b)   (c)
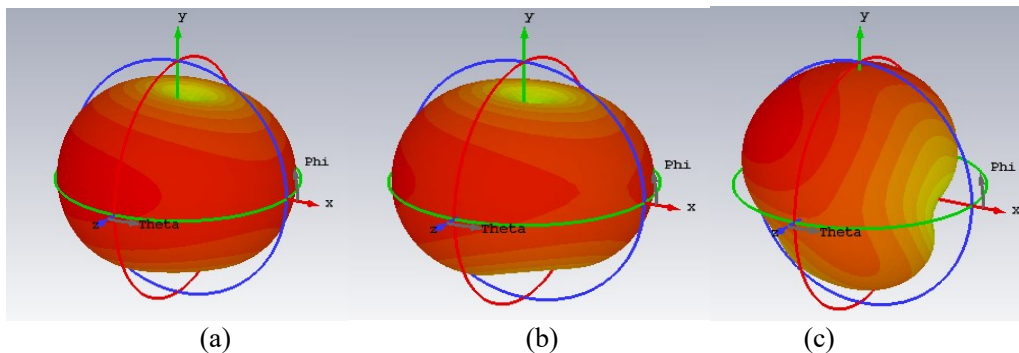
Fig. 20: 3D radiation pattern of Antenna 5 at (a) 2.448 GHz, (b) 2.864 GHz, (c) 5.8 GHz.

3.3 Gain and Directivity

The gain for both designs were determined based on the realized gain where it is the actual gain that considers the total efficiency of the antenna [1]. The realized gains of Antenna 4 were -12.38 dBi, -1.272 dBi, and -4.065 dBi at 2.4 GHz, 4.44 GHz, and 5.8 GHz, while Antenna 5 had realized gains of 1.110 dBi, 1.382 dBi, and 2.829 dBi at 2.448 GHz, 2.864 GHz, and 5.8 GHz. It can be inferred that Antenna 5, at resonant frequency of 5.8 GHz, had the most gain from the radiation at the main lobe and all gains of Antenna 5 were positive.

The directivity of the antenna indicates the ratio of maximum radiation intensity to the average radiation intensity in a specified direction [1]. Antenna 4 had a main lobe directivity of 2.183 dBi, 2.563 dBi, and 1.005 dBi at respective resonant frequencies of 2.4 GHz, 4.44 GHz, and 5.8 GHz. As for Antenna 5, that operated as multi-band antenna at 2.448 GHz, 2.864 GHz, and 5.8 GHz, it had main lobe directivity of 2.462 dBi, 2.765 dBi, and 4.231 dBi respectively. Hence, Antenna 5 had the highest directivity in the main lobe direction compared to Antenna 4.

Based on the simulation results, Antenna 5 had better performance compared to Antenna 4 because it had good impedance matching, greater gain, wider bandwidth, and had an omnidirectional pattern.

3.4 Comparison of Simulated and Measured Result

The fabricated Antenna 4 had three operating bands at 2.326 GHz, 4.408 GHz, and 5.806 GHz with good return loss below -10 dB where it indicates that this antenna only manages to resonate at targeted frequency of 5.8 GHz, as illustrated in Fig. 21. Moreover, the measured resonant frequencies of the antenna were shifted to smaller frequency than the simulated resonant frequencies due to the loss from the SMA connector that affects its performance. Figure 23 illustrates the comparison between the simulated and measured result of Antenna 4 where they almost correspond to each other.

Figure 22 illustrates the measured return loss of Antenna 5 where the fabricated antenna resonated at 3.388 GHz, 5.848 GHz, and 6.058 GHz with a good return loss below -10 dB. However, it was not fully correlated with the simulated return loss as depicted in Fig.24. This is due to the defective structure of the antenna produced during the chemical etching process that affects the antenna performance. Besides, multiple soldering attempts between the SMA connector and the antenna also caused excess heat to be applied to the board, which also had an impact on its performance. Therefore, it can be inferred that the measured results for both fabricated Antenna 4 and Antenna 5 were partially agreed with the simulated result.
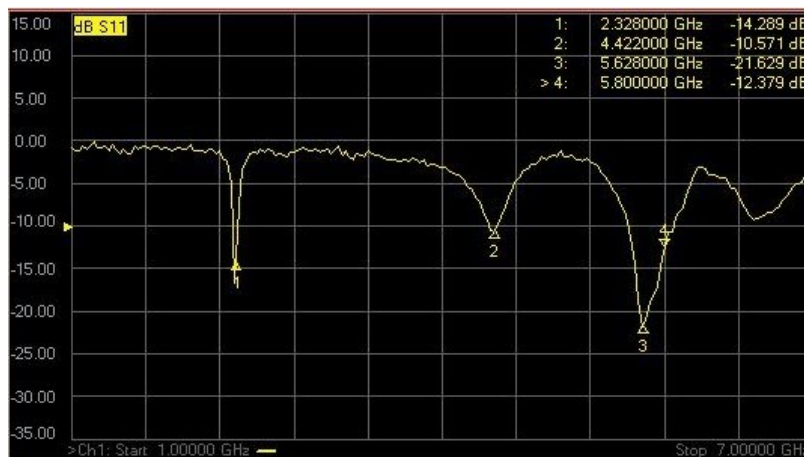
Fig. 21: Measured return loss of Antenna 4.
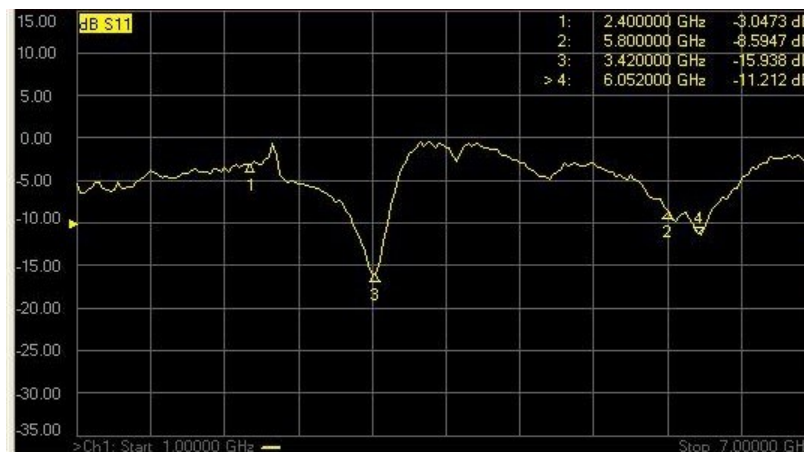
Fig. 22: Measured return loss of Antenna 5.
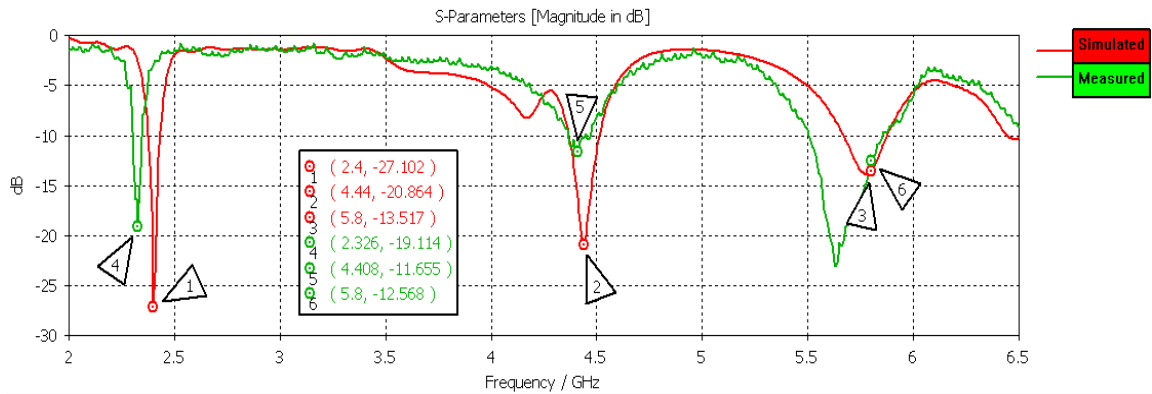
Fig. 23: Return loss comparison of simulated and measured Antenna 4.
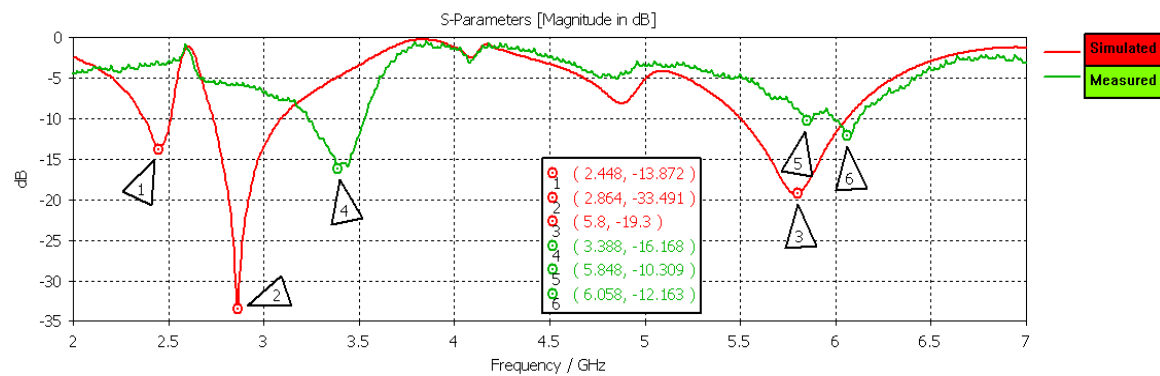
Fig. 24: Return loss comparison of simulated and measured Antenna 5.

Table 4 shows the comparison of the proposed designs (Antenna 4 and Antenna 5) to related works. It can be observed that all the works resonated at 2.4 GHz, which is the ISM band frequency that is commonly used by IoT applications. The proposed antenna designs in this paper had bigger size compared to work by [14]. However, the work by [14] only had one operating band which indicates that the proposed antenna designs had better performance with multi-band operation despite its size. Work by [15] had higher gain compared to the proposed antenna designs, but it only had one resonant frequency with bigger size. Moreover, work by [16] had the smallest antenna size and tri-band operation which is similar to the proposed antenna designs with three resonant frequencies. However, it did not resonate at 5.8 GHz, which is the required frequency for Wi-Fi application. Moreover, work by [17] had more bands of operation at five resonant frequencies, but its bandwidth is narrower and is of bigger size compared to proposed antenna design 2 that had wider bandwidth and smaller size.

Table 4: Comparison of proposed designs with related works

Ref.	Resonant frequency [GHz]	Size [mm^3]	Gain [dBi]	Bandwidth [MHz]
[14]	2.4	16 x 32.5 x 1.6	1.8	0.132
[15]	2.4	40 x 30 x 1.6	3.23	574
[16]	2.4, 3.5, 6.7	20 x 20 x 1.5	-	-
[17]	2.4, 2.7, 4.7, 5.6, 8.8	30 x 24.8 x 1.6	-	100, 130, 480, 350,210
Proposed 1	2.4, 4.44, 5.8	30 x 24.8 x 1.6	-12.38, -1.272, -4.065	54.5, 144.1, 204.9
Proposed 2	2.448, 2.864, 5.8	30 x 20 x 1.575	1.110, 1.382, 2.829	137.2, 350.9, 551.2

4. CONCLUSION

A miniaturized multi-band ring monopole antenna incorporated with RCSRR metamaterial structure as the radiating element and L-slotted ground plane, was successfully designed, simulated, measured, and analyzed. The antenna that resonated at 2.448 GHz, 2.864 GHz, and 5.8 GHz, and designed on Rogers RT5880 substrate, had a compact size with dimensions of 30 mm x 20 mm x 1.575 mm which indicates 57.8 % size reduction from conventional ring monopole antenna. The antenna had good impedance matching at -13.8 dB, -33.491 dB, and -19.3 dB, greater gain of 1.110 dBi, 1.382 dBi, and 2.829 dBi, wider bandwidth of 137.2 MHz, 250.9 MHz, and 551.2 MHz compared to the antenna that was designed on FR-4 substrate. It also had omnidirectional pattern which is suitable for use in the wireless connectivity that is essential for IoT applications. However, the measured result partially agreed with the simulation result where the fabricated antennas were unable to resonate at 2.4 GHz due to the defective antenna structure and the loss from the SMA connector and soldering process that affect its performance. Hence, the measured result was unable to fully validate the simulated result of the antenna. For future work, it is suggested to fabricate the miniaturized antenna with a laser etching method to ensure that a good antenna structure is produced. Besides, the antennas can also be miniaturized by incorporating different metamaterial structure such as electromagnetic bandgap (EGB) to broaden the research on miniaturized antenna using metamaterials.

ACKNOWLEDGEMENT

REFERENCES

[1] Balanis CA. (2016) Antenna Theory: Analysis and Design. 4th Edition. New York, Wiley.
[2] Wi-Fi certified 6 [https://www.wi-fi.org/discover-wi-fi/wi-fi-certified-6].
[3] Rothwell EJ, Ouedraogo RO. (2014) Antenna miniaturization: definitions, concepts, and a review with emphasis on metamaterials. Journal of Electromagnetic Waves and Application, 28(17): 2089-2123.
[4] Cheng K, Liang Z, Hu B. (2021) Design of Miniaturized Microstrip Antenna for Smart Home Wireless Sensor. In Proceedings of the 2021 IEEE 4th International Conference on Electronic Information and Communication Technology (ICEICT): 18-20 Aug 2021; , pp. 234-236, Xi'an, China. pp 234-236. doi: 10.1109/ICEICT53123.2021.953 1163.
[5] Chandan K. (2020) Truncated ground plane multiband monopole antenna for WLAN and WiMAX applications. IETE Journal of Research. 68(4): 2416-2421. https://doi.org/10.1080/03772063.2019.1709568
[6] Bhatia SS, Sharma N. (2020) A Compact Wideband Antenna Using Partial Ground Plane with Truncated Corners, L–Shaped Stubs and Inverted T–Shaped Slots. Progress In Electromagnetics Research M. 97: 133-144. doi:10.2528/pierm20072503
[7] Chandan, Barthi G, Srivastava T, Rai BS. (2018) Dual band monopole antenna for WLAN 2.4/5.2/5.8 with truncated ground. In Proceedings of AIP, 1952(1). AIP Publishing LLC, https://doi.org/10.1063/1.5031998
[8] Baudha S, Basak A, Manocha M, Yadav MV. (2020) A compact planar antenna with extended patch and truncated ground plane for ultra-wide band application. Microwave and Optical Technology Letters 62(1): 200-209. https://doi.org/10.1002/mop.31988

[9]   Rahardi R, Rizqi M, Lukito WD, Wibowo R, Oktafiani F, Munir A. (2020) Reduced Size Meander Line-based 433MHz Printed Dipole Antenna for UAV Telemetry Application. In Proceedings of International Conference on Radar, Antenna, Microwave, Electronics, and Telecommunications (ICRAMET), pp. 176-179.
doi: 10.1109/ICRAMET51080.2020.9298675

[10]   Ezhumalai A, Ganesan N, Balasubramaniyan S. (2021) An extensive survey on fractal structures using iterated function system in patch antennas. International Journal of Communication Systems. 34(15): e4932. https://doi.org/10.1002/dac.4932

[11]   Chourasia S, Sharma SK, Goswami DP. (2020) Review on miniaturization techniques of microstrip patch antenna. In Proceedings of the 4th International Conference: Innovative Advancement in Engineering & Technology (IAET). http://dx.doi.org/10.2139/ssrn.3550995

[12]   Manage PS, Naik U, Nargundkar S, Rayar V. (2020) A Survey on applications of Metamaterials in Antenna Design. In Proceedings of Third International Conference on Smart Systems and Inventive Technology: 20-22 August 2020; Tirunelveli, India. IEEE; pp. 153-158. doi: 10.1109/ICSSIT48917.2020.9214088

[13]   Mishra RN, Arora A, Singh S, Bhattacharyya S. (2017) A split ring resonator (SRR) based metamaterial structure for bandstop filter applications. In Proceedings of IEEE Applied Electromagnetics Conference (AEMC): 19-22 December 2017; Aurangabad, India. IEEE; pp. 1-2. doi: 10.1109/AEMC.2017.8325685.

[14]   Al-Bawri SS, Jamlos MF. (2018) Design of Low-Profile Patch Antenna Incorporated with Double Negative Metamaterial Structure. In Proceedings of International RF and Microwave Conference (RFM): 17-19 December 2018; Penang, Malaysia, IEEE; pp. 45-48.
doi: 10.1109/RFM.2018.8846501

[15]   Geetharamani G, Aathmanesan T. (2020) Design of Metamaterial Antenna for 2.4 GHz WiFi Applications. Wireless Personal Communication 113: 2289-2300. https://doi.org/10.1007/s11277-020-07324-z

[16]   Lou R, Mohammad K, Naser-Moghadasi M, Sadeghzadeh RA. (2017) Compact multi-band circularly polarized CPW fed antenna based on metamaterial resonator. Wireless Personal Communications 94(4): 2853-2863. https://doi.org/10.1007/s11277-016-3722-x

[17]   Ali T, Mohammad Saadh AW, Biradar RC, Anguera J, Andújar A. (2017) A miniaturized metamaterial slot antenna for wireless applications. AEU - International Journal of Electronics and Communications, 82: 368-382. https://doi.org/10.1016/j.aeue.2017.10.005

[18]   CST Studio Suite 3D EM simulation and analysis software [https://www.3ds.com/products-services/simulia/products/cst-studio-suite]

[19]   Muneer B, Shaikh FK, Zhu Q. (2020) Antennas for IoT application: An RF and microwave aspect of IoT. In IoT Architectures, Models, and Platforms for Smart City Applications. Hershey, PA: IGI Global, 2020: 180-192. doi: 10.4018/978-1-7998-1253-1.ch009

[20]   Lizzi L, Ferrero F, Monin P, Danchesi D, Boudaud S. (2016) Design of miniature antennas for IoT applications. In Proceedings of Sixth International Conference on Communications and Electronics (ICCE): 27-29 July 2016; Ha-Dong, Vietnam, IEEE, pp. 234-237.
doi: 10.1109/CCE.2016.7562642.

[21]   Elijah AA, Mokayef M. (2020) Miniature microstrip antenna for IoT application. In Proceedings of Materials Today, 29: 43-47. https://doi.org/10.1016/j.matpr.2020.05.678

[22]   Al-Sehemi A, Al-Ghamdi A, Dishovsky N, Atanasova G, Atanasov N. (2020) A flexible broadband antenna for IoT applications. International Journal of Microwave and Wireless Technologies: 12(6): 531-540. https://doi.org/10.1017/S1759078720000161

[23]   Palhade SM, Yawale SP. (2015) Design and Photo-Lithographic Fabrication of Microstrip Patch Antenna. International Journal of Science and Research (IJSR), 4(2): 2021-2024. https://www.ijsr.net/get_abstract.php?paper_id=SUB151708